ARTICLE OPEN

Check for updates

Genomic and transcriptomic determinants of clinical outcomes in patients with AML and *DNMT3A* mutations

Sao-Chih Ni[1], Chi-Yuan Yao[2,3,4], Xavier Cheng-Hong Tsai[2], Min-Yen Lo[3,5], Chien-Yuan Chen[6], Wan-Hsuan Lee[3,6], Chien-Chin Lin[2,4], Yuan-Yeh Kuo[7], Yen-Ling Peng[2], Mei-Hsuan Tseng[7], Yu-Sin Wu[8], Ming-Chih Liu[9], Liang-In Lin[10], Ming-Kai Chuang[2,4], Bor-Sheng Ko[1,2], Ming Yao[2], Jih-Luh Tang[1,2,7], Feng-Ming Tien[2,3]✉, Wen-Chien Chou[2,4], Hsin-An Hou[2,11] and Hwei-Fang Tien[2,12]

Acute myeloid leukemia (AML) and *DNMT3A* mutations (*DNMT3A*^{mut}) are considered to carry intermediate risk under the 2022 European LeukemiaNet (ELN-2022) classification in the absence of other co-mutations or cytogenetic abnormalities. However, this group is highly heterogeneous. In this study, the genomic and transcriptomic features influencing outcomes in *DNMT3A*-mutated AML were examined in a cohort of 884 patients with AML receiving standard chemotherapy. Stratification by *NPM1* and *FLT3*-ITD status revealed worse survival among patients with *NPM1* mutations and wild-type *FLT3*-ITD (*NPM1*^{mut}/*FLT3*-ITD^{wt}) than patients in the ELN-2022 favorable risk group. The other three subgroups (*NPM1*^{mut}/*FLT3*-ITD^{mut}, *NPM1*^{wt}/*FLT3*-ITD^{mut}, and *NPM1*^{wt}/*FLT3*-ITD^{wt}) exhibited worse prognoses than patients in the ELN-2022 intermediate risk group. Additionally, the presence of *TET2*^{mut} in patients with AML and *DNMT3A*^{mut}/*NPM1*^{mut}/*FLT3*-ITD^{wt} led to reclassification from favorable risk to intermediate risk in the ELN-2022. RNA-sequencing analysis revealed a distinct transcriptomic profile in patients with *TET2*^{mut}, highlighting the enrichment of leukemic stem cell signatures and dendritic cell migration, with *MMP14*, *CD200*, and *CT45A5* identified as key differentially expressed genes. In conclusion, co-mutation patterns strongly affected AML outcomes in patients with *DNMT3A*^{mut}. Patients with *TET2*^{mut} constituted a unique subgroup within the ELN-2022 favorable *DNMT3A*^{mut}/*NPM1*^{mut}/*FLT3*-ITD^{wt} group, characterized by distinct transcriptomic features and an unfavorable prognosis.

Blood Cancer Journal (2025)15:97 ; https://doi.org/10.1038/s41408-025-01287-9

INTRODUCTION

DNMT3A encodes the DNA methyltransferase 3 alpha enzyme, which adds methyl groups to cytosine residues in CpG dinucleotides [1]. This process is essential for gene expression regulation and the maintenance of genomic stability. Mutations in *DNMT3A* (*DNMT3A*^{mut}) have been identified in approximately 14–22% of patients with acute myeloid leukemia (AML) [1–5], with a higher prevalence of 29–34% observed in those with normal karyotype AML [6, 7]. Numerous studies have demonstrated a correlation between *DNMT3A*^{mut} and poorer survival outcomes [1, 2, 8–11]. However, the prognostic implications of *DNMT3A*^{mut} remain uncertain, because these mutations frequently exist alongside other genetic alterations, hindering identification of their independent effects on clinical outcomes. Notably, *DNMT3A*^{mut} is not listed as a major prognostic factor in the 2022 European Leukemia Net (ELN-2022) classification [12].

Most *DNMT3A*^{mut} appear alongside other molecular abnormalities, such as *FLT3*-ITD, *NPM1*, and *IDH1*, underscoring the clinical heterogeneity among individuals with these mutations. *NPM1* mutations (*NPM1*^{mut}) have exhibited a strong association with favorable outcomes, whereas *FLT3*-ITD mutations (*FLT3*-ITD^{mut}) have been linked to poorer outcomes [13, 14]. However, the prognostic implications of other concurrent mutations in patients with AML and *DNMT3A*^{mut} require further clarification. Moreover, the transcriptomic features that affect survival in patients with *DNMT3A*^{mut} remain poorly understood, indicating a need for additional research. Dysregulated pathways that function independently of specific mutational backgrounds should be elucidated to uncover new opportunities for therapeutic intervention. In this study, we performed a detailed subgroup analysis of clinical heterogeneity in patients with AML and *DNMT3A*^{mut} based on

[1]Department of Hematological Oncology, National Taiwan University Cancer Center, Taipei, Taiwan. [2]Division of Hematology, Department of Internal Medicine, National Taiwan University Hospital, Taipei, Taiwan. [3]Graduate Institute of Clinical Medicine, College of Medicine, National Taiwan University, Taipei, Taiwan. [4]Department of Laboratory Medicine, National Taiwan University Hospital, Taipei, Taiwan. [5]Division of Hematology, Department of Internal Medicine, National Taiwan University Hospital Yunlin Branch, Yunlin, Taiwan. [6]Department of Internal Medicine, National Taiwan University Hospital, Hsin-Chu Branch, Hsin-Chu, Taiwan. [7]Tai-Chen Cell Therapy Center, National Taiwan University, Taipei, Taiwan. [8]Department of Nursing, National Taiwan University Hospital, Taipei, Taiwan. [9]Department of Pathology, National Taiwan University Hospital, Taipei, Taiwan. [10]Department of Clinical Laboratory Sciences and Medical Biotechnology, College of Medicine, National Taiwan University, Taipei, Taiwan. [11]Division of General Medicine, Department of Internal Medicine, National Taiwan University Hospital, Taipei, Taiwan. [12]Department of Internal Medicine, Far-Eastern Memorial Hospital, New Taipei City, Taiwan. ✉email: b92401007@ntu.edu.tw

Received: 13 February 2025 Revised: 9 April 2025 Accepted: 14 April 2025
Published online: 20 May 2025

comprehensive genomic and transcriptomic data. Our findings were also thoroughly validated in several external cohorts.

METHODS AND MATERIALS

Sample

A total of 884 newly diagnosed patients with de novo non-M3 AML who received standard chemotherapy at National Taiwan University Hospital (NTUH) were enrolled in this study. AML diagnosis and classification were performed according to the International Consensus Classification [15] and the 5th World Health Organization Classification [16]. Detailed patient characteristics and treatment regimens are provided in the supplementary data [17].

Ethics approval and consent to participate

All methods were performed in accordance with the relevant guidelines and regulations. Live vertebrates were not used in this project. The study was approved by the NTUH institutional review board, and written informed consent was obtained from all participants in accordance with the Declaration of Helsinki (approval number 201709072RINC and 202109078RINB).

Cytogenetics

Chromosomal analyses were performed according to a procedure described in a previous study [18]. Karyotypes were classified on the basis of risk groups defined by the Medical Research Council [19].

Mutation analysis

We performed targeted next generation sequencing (NGS) with a TruSight myeloid sequencing panel (Illumina, San Diego, CA, USA) to analyze mutations in 15 full exon genes and 39 oncogenic hotspot genes. A HiSeq platform (Illumina, San Diego, CA, USA) with a median reading depth of 12,000× was used for sequencing. Due to the suboptimal sequencing sensitivity of this method, *CEBPA* mutations were confirmed through Sanger sequencing. *FLT3*-ITD was analyzed through polymerase chain reaction (PCR) followed by fluorescence capillary electrophoresis. *KMT2A*-PTD was analyzed through PCR followed by Sanger sequencing [20].

RNA sequencing analysis

Bone marrow (BM) mononuclear cells were obtained from 264 patients with AML, including 80 with *DNMT3A*^{mut} and 184 with wild-type *DNMT3A* (*DNMT3A*^{wt}) and normal karyotypes. The BM samples were then analyzed through RNA sequencing (RNA-seq) per the method of a previous study [21]. RNA was processed into sequencing libraries with the TruSeq Stranded mRNA Library Prep Kit (Illumina, San Diego, CA, USA) and sequenced on an Illumina NovaSeq 6000 sequencing system (150 bp paired-end). Reads were trimmed with Cutadapt (v2.3), aligned to GRCh38.p12 using STAR (v2.6.1a) [22], and quantified with Gencode annotations (v28) [23]. Read counts were normalized across all samples according to the trimmed mean of M-values with the *calcNormFactors* function of the *edgeR* package in R software [24]. Gene expression was calculated in terms of $\log_2(\mathrm{CPM}+1)$ (counts per million reads) for further analysis. We used the *limma* package in R to identify differentially expressed genes (DEGs) and determined log2 fold changes (logFC) and false discovery rate (FDR)-adjusted *P* values using the Benjamini–Hochberg method.

We conducted analyses of gene ontology to investigate the enrichments of expression profiles associated with *DNMT3A*^{mut} in gene sets curated in the Molecular Signatures Database (MSigDB) [25]. The statistical significance of the degree of enrichment was assessed through a random permutation test with 1000 repetitions [26].

External datasets

We downloaded AML RNA-seq data from the Cancer Genome Atlas (TCGA) generated with the Illumina HiSeq 2000 platform ($n = 173$) and Beat-AML RNA-seq data for validation [27, 28]. The prognostic relevance of concurrent mutations was further validated on the basis of patient data with molecular annotations from the German–Austrian Acute Myeloid Leukemia Study Group (AMLSG, $n = 1540$) and the UK National Cancer Research Institute (UK-NCRI) trials ($n = 2113$) [4, 29].

Statistical analysis

Chi-square tests were performed for comparisons of discrete variables. If the expected contingency table values were below 5, Fisher's exact test was performed. Mann–Whitney U tests were performed to compare continuous variables and the medians of distributions. Overall survival (OS) was defined as the time from initial diagnosis to the date of last follow-up or death from any cause. Event-free survival (EFS) was defined as the time from diagnosis to the first instance of the following: treatment failure, relapse after first complete remission (CR1), or death from any cause. Disease-free survival (DFS) was defined as the time from diagnosis to either relapse or death from any cause [30]. A P value < 0.05 indicated statistical significance. The effect of allogeneic hematopoietic stem cell transplantation (allo-HSCT) at CR1 on outcomes in patients with *DNMT3A*^{mut} was assessed according to the Mantel–Byar approach, and results were visualized in Simon–Makuch plots [31]. Statistical analyses were performed with SPSS 23 (SPSS, Chicago, IL, USA) and R software 4.3.1 (R Foundation for Statistical Computing, Vienna, Austria).

RESULTS

Patient characteristics and clinical outcomes

DNMT3A^{mut} was identified in 16.2% of the 884 patients in our cohort (143) (Supplementary Table 1). The median age of patients with *DNMT3A*^{mut} was 53 years (range: 17–82 years), significantly higher than that of patients with *DNMT3A*^{wt}. Patients with *DNMT3A*^{mut} also had significantly higher white blood cell counts, platelet counts, and hemoglobin levels at diagnosis. Cytogenetic analysis revealed a significantly higher proportion of patients with *DNMT3A*^{mut} had intermediate risk profiles than those with *DNMT3A*^{wt} (93.0% vs. 72.1%, respectively, $P < 0.001$). Patients with *DNMT3A*^{mut} had a higher incidence of *NPM1*^{mut} but a lower incidence of AML with core-binding factor positivity, *CEBPA* mutations, and *KMT2A* rearrangements (Table 1).

CR1 rates were comparable between patients with *DNMT3A*^{mut} and *DNMT3A*^{wt} (74.1 vs. 75.8%, respectively, $P = 0.662$). Among patients who did not receive allo-HSCT at CR1, relapse rates remained comparable between both groups (40.6% vs. 32.0%, $P = 0.102$). Patients with *DNMT3A*^{mut} exhibited similar OS and EFS as those in the ELN-2022 intermediate risk group (Fig. 1A). Patients in this cohort with *DNMT3A*^{wt} had significantly better OS and EFS than those with *DNMT3A*^{mut} after a median follow-up time of 7.3 years (median OS 30.1 vs. 21.3 months, respectively, $P = 0.005$; median EFS 12.6 vs. 7.4 months, $P = 0.009$) (Fig. 1B).

Frequency and prognostic relevance of concurrent mutations in *DNMT3A*^{mut}

At least one concurrent mutation was identified in most patients with *DNMT3A*^{mut} (97.2%) (Fig. 2A). The most frequently mutated genes were *NPM1* (52.8%), *FLT3*-ITD (30.6%), *IDH2* (26.4%), *FLT3*-TKD (15.3%), *IDH1* (10.4%), and *PTPN11* (9.7%) (Fig. 2B, Supplementary Table 2). Given the well-established prognostic significance of *NPM1*^{mut} and *FLT3*-ITD^{mut}, we stratified patients with *DNMT3A*^{mut} into four subgroups by whether these two genetic alterations were present. To further strengthen risk stratification, we also assessed the prognostic effects of concurrent mutations within each subgroup. Patients with *DNMT3A*^{mut} and different *NPM1* and *FLT3*-ITD mutation statuses differed significantly in OS ($P = 0.004$) and EFS ($P = 0.009$) (Fig. 2C). Outcomes were significantly better among *DNMT3A*^{mut} patients with *NPM1*^{mut} and wild-type *FLT3*-ITD (*FLT3*-ITD^{wt}) than in patients with *NPM1*^{mut}/*FLT3*-ITD^{mut}, *NPM1*^{wt}/*FLT3*-ITD^{mut}, or *NPM1*^{wt}/*FLT3*-ITD^{wt}, in which prognoses were similarly poor. Furthermore, outcomes were significantly worse in the *NPM1*^{mut}/*FLT3*-ITD^{wt} subgroup than in the ELN-2022 favorable risk group (median OS, 97.8 months vs. not reached, $P = 0.047$; median EFS, 18.0 vs. 138.1 months, $P = 0.036$). The other three subgroups all exhibited worse outcomes than the ELN-2022 intermediate risk group (Supplementary Fig. 1A–D). These results indicate that outcomes among

Table 1. Comparison of clinical and laboratory features between AML patients with and without *DNMT3A* mutations.

Clinical characters	*DNMT3A*^{wt} ($n = 741$)	*DNMT3A*^{mut} ($n = 143$)	*P* value
Sex			0.098
Female	338	76	
Male	403	67	
Age	48 (12–84)	53 (17–82)	<0.001
Laboratory data			
WBC, $\times 10^9$ /L	15.4 (0.16–627.8)	34.6 (0.49–315.1)	<0.001
Hb, g/dL	8.1 (2.4–15)	8.6 (3.7–15.3)	0.024
Platelet, $\times 10^9$ /L	42 (3–1017)	60 (2–514)	<0.001
PB blast (%)	42 (0–99)	35 (0–99)	0.876
LDH (U/L)	680 (96–15000)	653 (111–7177)	0.944
Cytogenetics			
Favorable	123 (16.6)	2 (1.4)	<0.001
Intermediate	534 (72.1)	133 (93.0)	<0.001
Unfavorable	77 (10.4)	5 (3.5)	0.009
NA	7 (1.0)	3 (1.4)	0.233
2022 ICC			
t(8;21)(q22;q22.1)/*RUNX1::RUNX1T1*	87 (11.7)	1 (0.7)	<0.001
inv(16)(p13.1q22) or t(16;16)(p13.1;q22)/*CBFB::MYH11*	38 (5.1)	1 (0.7)	0.018
t(9;11)(p21.3;q23.3)/*MLLT3::KMT2A*	12 (1.6)	0 (0.0)	0.125
other *KMT2A* rearrangements	27 (3.6)	0 (0.0)	0.020
t(6;9)(p22.3;q34.1)/*DEK::NUP214*	5 (0.7)	0 (0.0)	0.325
inv(3)(q21.3q26.2) or t(3;3)(q21.3;q26.2)/*GATA2; MECOM(EVI1)*	11 (1.5)	0 (0.0)	0.125
t(9;22)(q34.1;q11.2)/*BCR::ABL1*	3 (0.4)	1 (0.7)	0.818
CEBPA$^{bZIP\text{-}inf}$	107 (14.4)	5 (3.5)	<0.001
Mutated *NPM1*	99 (13.4)	72 (50.3)	<0.001
Mutated *TP53*	34 (4.6)	2 (1.4)	0.077
AML with myelodysplasia-related gene mutations	142 (19.2)	27 (18.9)	0.937
AML with myelodysplasia-related cytogenetic abnormalities	42 (5.7)	7 (4.9)	0.712
AML, NOS	134 (18.1)	27 (18.9)	0.821
2022 WHO			
RUNX1-RUNX1T1 fusion	87 (11.7)	1 (0.7)	<0.001
CBFB-MYH11 fusion	38 (5.1)	1 (0.7)	0.018
DEK-NUP214 fusion	5 (0.7)	0 (0.0)	0.325
BCR-ABL1 fusion	3 (0.4)	1 (0.7)	0.818
KMT2A rearrangement	39 (5.3)	0 (0.0)	0.005
MECOM rearrangement	11 (1.5)	0 (0.0)	0.143
NUP98 rearrangement	13 (1.8)	0 (0.0)	0.111
CEBPA mutation	112 (15.2)	6 (4.2)	<0.001
NPM1 mutation	99 (13.2)	72 (50.3)	<0.001
Myelodysplasia-related	163 (22.0)	25 (17.5)	0.227
AML, defined by differentiation	171 (23.1)	37 (25.9)	0.470
ELN-2022			
Favorable	285 (38.5)	43 (30.1)	0.057
Intermediate	176 (23.8)	56 (39.2)	<0.001
Unfavorable	280 (37.8)	44 (30.8)	0.111
CR1	562 (75.8)	106 (74.1)	0.662
Relapse (CR1 no HSCT)	238 (32.1)	58 (40.6)	0.102
Allo-HSCT	314 (42.4)	64 (44.8)	0.598
CR1	154 (20.8)	29 (20.3)	0.892
CR2	66 (8.9)	8 (5.6)	0.190
Others	94 (12.7)	27 (18.9)	0.048

Allo-HSCT allogeneic hematopoietic stem cell transplantation, *CR* complete remission, *ELN* European LeukemiaNet, *Hb* hemoglobin, *PB* peripheral blood, *ICC* International Consensus Classification, *LDH* lactate dehydrogenase, *NA* not available, *WBC* white blood cell, *WHO* World Health Organization.

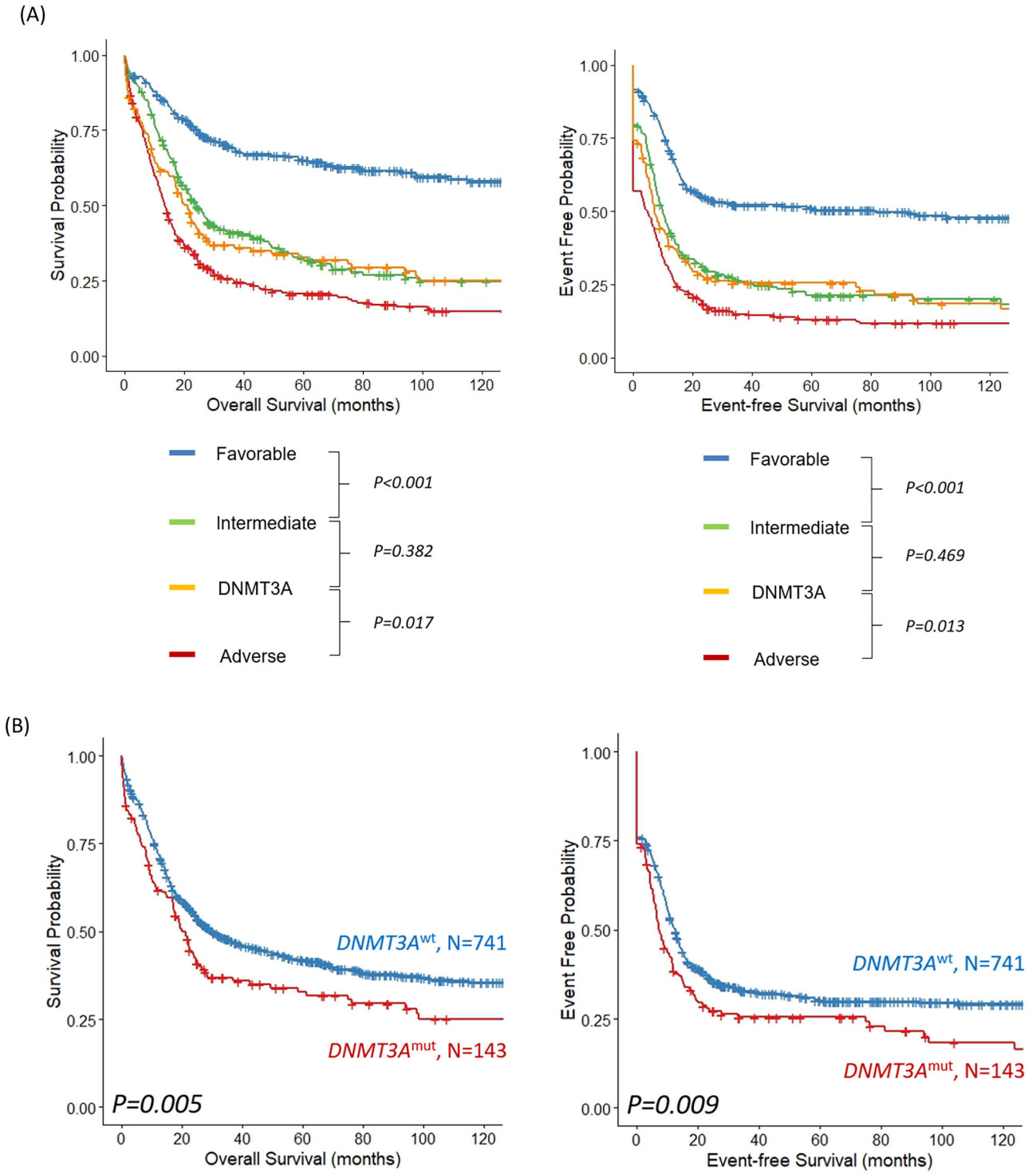

Fig. 1 Survival outcomes in patients with *DNMT3A*^{mut}. A Comparison of Kaplan–Meier survival curves for OS and EFS among patients with AML stratified according to ELN-2022 risk groups (favorable, intermediate, adverse) and *DNMT3A* mutation status. OS and EFS for the *DNMT3A*^{mut} group closely aligned with those of the ELN-2022 intermediate risk group. **B** *DNMT3A*^{mut} were associated with significantly worse OS and EFS than *DNMT3A*^{wt}.

all patients with *DNMT3A*^{mut} were inferior to those predicted under the current ELN-2022 risk categories.

The highest frequency of co-mutations was observed in the *NPM1*^{mut}/*FLT3*-ITD^{wt} group, including *FLT3*-TKD (25.5%), *IDH2* (19.1%), *PTPN11* (17.0%), *NRAS* (14.9%), and *TET2* (14.9%). Stratification according to these co-mutations revealed that *TET2* mutations (*TET2*^{mut}) were associated with the lowest survival rates (Fig. 2D). Notably, in our analysis of patients based on ELN-2022 risk stratification, those with *TET2*^{mut} exhibited significantly worse OS and a trend towards inferior EFS than patients in the ELN-2022 favorable risk group (median OS, 22.9 months vs. not reached, $P = 0.008$; median EFS, 11.8 vs. 138.2 months, $P = 0.054$) (Fig. 2E). Patients in our cohort with *TET2*^{mut} shared similar OS and EFS with the ELN-2022 intermediate risk group (Supplementary Fig. 2A). By

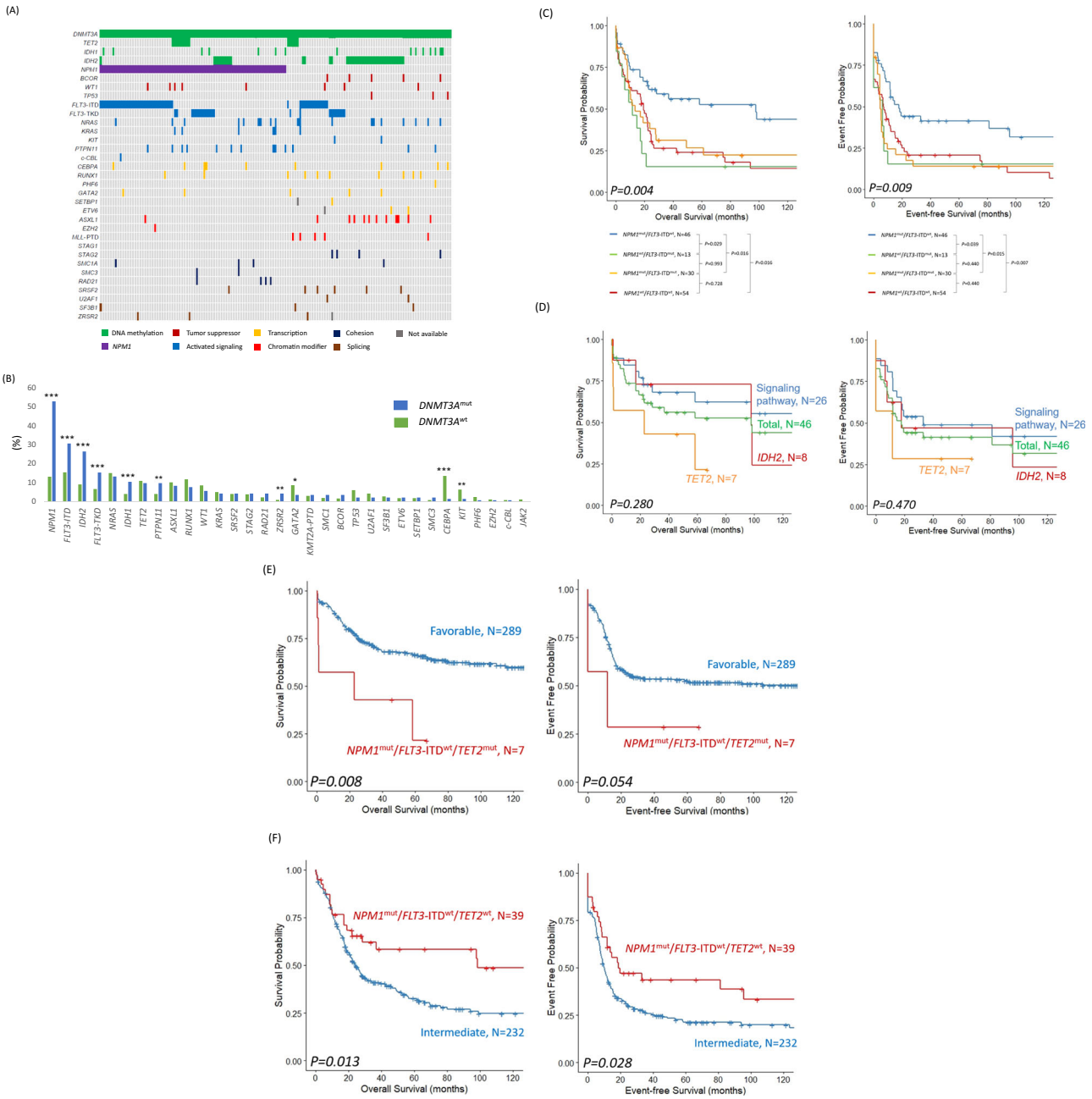

Fig. 2 Prevalence and prognostic implications of concurrent mutations in patients with *DNMT3A*^{mut}. **A** Oncoprint of recurrent genetic mutations in patients with *DNMT3A*^{mut} and AML. Colored bars represent mutations, categorized according to functional gene classes. **B** Prevalence of concurrent mutations in patients with *DNMT3A*^{mut} and *DNMT3A*^{wt}. Mutations observed in at least 1% of patients in one subgroup are displayed. Significant differences between *DNMT3A*^{mut} and *DNMT3A*^{wt} groups are marked as follows: $^{*}P < 0.05$, $^{**}P < 0.01$, $^{***}P < 0.001$. **C** OS and EFS of patients with *DNMT3A*^{mut} stratified according to *NPM1* and *FLT3*-ITD status. Patients with *NPM1*^{mut}/*FLT3*-ITD^{wt} exhibited significantly better OS and EFS than those in other groups. **D** OS and EFS in the *DNMT3A*^{mut}/*NPM1*^{mut}/*FLT3*-ITD^{wt} group, stratified according to concurrent genetic mutations: *TET2*, *IDH2*, signaling pathway mutations (*PTPN11*, *FLT3*-TKD, and *NRAS*), and total subgroup patients. The worst outcomes were observed in the *DNMT3A*^{mut}/*NPM1*^{mut}/*FLT3*-ITD^{wt}/*TET2*^{mut} subgroup. **E** OS and EFS comparison between the *DNMT3A*^{mut}/*NPM1*^{mut}/*FLT3*-ITD^{wt}/*TET2*^{mut} subgroup and ELN-2022 favorable risk group. Worse outcomes were observed in the *DNMT3A*^{mut}/*NPM1*^{mut}/*FLT3*-ITD^{wt}/*TET2*^{mut} subgroup. **F** OS and EFS comparison between the *DNMT3A*^{mut}/*NPM1*^{mut}/*FLT3*-ITD^{wt}/*TET2*^{wt} subgroup and ELN-2022 intermediate risk group. Better outcomes were observed in the *DNMT3A*^{mut}/*NPM1*^{mut}/*FLT3*-ITD^{wt}/*TET2*^{wt} subgroup.

contrast, among patients without *TET2*^{mut}, OS and EFS were higher relative to patients in the ELN-2022 intermediate risk group (median OS, 98.2 vs. 24.2 months, $P = 0.013$; median EFS, 18.7 vs. 10.7 months, $P = 0.028$) (Fig. 2F) and similar relative to patients in the ELN-2022 favorable risk group (Supplementary Fig. 2B). The *DNMT3A*^{mut}/*NPM1*^{mut}/*FLT3*-ITD^{wt}/*TET2*^{mut} group exhibited a trend towards worse OS comparing with the *DNMT3A*^{mut}/*NPM1*^{mut}/*FLT3*-ITD^{wt}/wild-type *TET2* (*TET2*^{wt}) group (median, 22.9 vs. 98.2 months, respectively, $P = 0.097$) (Supplementary Fig. 2C). In patients with *DNMT3A*^{mut}/*NPM1*^{mut}/*FLT3*-ITD^{wt}/*PTPN11*^{wt}/*IDH2*^{wt}, *TET2*^{mut} were associated with significantly worse OS (*TET2*^{mut}, median, 1.3 months vs. not reached, $P = 0.024$) and a trend toward worse EFS (*TET2*^{mut}, median, 0.001 vs. 33.2 months, $P = 0.090$) (Supplementary Fig. 2D).

In the *NPM1*^{mut}/*FLT3*-ITD^{mut} group, frequent co-mutations were observed in myeloid dysplasia related genes (MDS-R, 16.6%), including *ASXL1, BCOR, EZH2, RUNX1, SF3B1, SRSF2, STAG2, U2AF1*, and *ZRSR2*, and in signaling pathways (13.3%). MDS-R genes were most frequently detected in the *NPM1*^{wt}/*FLT3*-ITD^{mut} group (9.3%), whereas the proportion of other co-mutations remained low. Notably, no significant differences in OS or EFS were observed within each group when stratified according to the type of co-mutations (Supplementary Fig. 2E, F). A high frequency of co-mutations was observed in the *NPM1*^{wt}/*FLT3*-ITD^{wt} group, including *IDH2* (48.1%), MDS-R genes (44.4%), and *NRAS* (16.7%). Patients with MDS-R genes were classified within the ELN-2022 unfavorable group and had a 5-year survival rate of approximately 25–30% [23]. Even patients with *DNMT3A*^{mut}/*NPM1*^{wt}/*FLT3*-ITD^{wt} who lacked MDS-R gene mutations were associated with poor survival outcomes that were similar to those of patients with MDS-R gene mutations, indicating the negative prognostic effects of *DNMT3A*^{mut} (Supplementary Fig. 2G). Patients with *IDH2* mutations were excluded for further stratification of the *NPM1*^{wt}/*FLT3*-ITD^{wt}/*IDH2*^{wt} group according to *NRAS* mutation status, which revealed that patients with *NRAS* mutations had better OS (median, not reached vs. 12.4 months, $P = 0.045$) (Supplementary Fig. 2H).

Effects of Allo-HSCT at CR1 in patients with *DNMT3A*^{mut}

Outcomes among patients with *DNMT3A*^{mut}, irrespective of their *NPM1* and *FLT3*-ITD mutation status, were inferior to those predicted under the current ELN-2022 risk categories. We also examined whether allo-HSCT at CR1 alleviated the poor survival of patients with *DNMT3A*^{mut}. Among these patients, 64 (44.8%) underwent allo-HSCT, with 29 (20.3%) receiving allo-HSCT at CR1. Among patients who received allo-HSCT at CR1, 12 had *NPM1* mutations and 10 had available *NPM1* PCR data before HSCT. *NPM1* was detected in 5 (50%) of these patients before the transplant (Supplementary table 3). To accurately evaluate the effects of allo-HSCT at CR1, we performed a Mantel–Byar analysis and constructed Simon–Makuch plots. Significantly better OS (median, 209.1 vs. 23.1 months, $P = 0.001$) and DFS (median, not reached vs. 10.2 months, $P < 0.001$) was observed among patients who received allo-HSCT at CR1 (Supplementary Fig. 3A). Among patients in the ELN-2022 favorable group with *DNMT3A*^{mut}/*NPM1*^{mut}/*FLT3*-ITD^{wt}, allo-HSCT at CR1 was associated with significantly improved DFS (median, not reached vs. 93.9 months, $P = 0.037$) but a nonsignificant difference in OS (median, not reached vs. 241.8 months, $P = 0.196$) compared with post-remission chemotherapy (Supplementary Fig. 3B).

External validation of survival outcomes stratified according to co-mutations in patients with AML and *DNMT3A*^{mut}

We integrated data from the AMLSG and UK-NCRI trial cohorts to analyze the prognostic effects of co-mutations (Supplementary Table 4). In the *DNMT3A*^{mut}/*NPM1*^{mut}/*FLT3*-ITD^{wt}/*PTPN11*^{wt}/*IDH2*^{wt} subgroup, *TET2*^{mut} were associated with significantly worse OS (*TET2*^{mut}, median, 2.9 years vs. not reached, $P = 0.020$) (Supplementary Fig. 4), consistent with findings from our cohort.

Characteristics and clinical outcomes of patients with *DNMT3A*^{mut} in relapse

Among patients with *DNMT3A*^{mut}, 63 (44.1%) experienced a relapse, and 34 (54.0%) of all relapsed patients achieved a second complete remission (CR2) after salvage reinduction chemotherapy (Supplementary Table 5). *FLT3*-ITD and *WT1* mutations were associated with a significantly lower likelihood of CR2 (*FLT3*-ITD, 38% vs. 72%, $P = 0.045$; *WT1*, 0% *vs.* 100%, $P = 0.012$). The median OS from the time of relapse was 10.5 months. Subsequent allo-HSCT was administered to 30 patients, including 12 at CR2. Patients who received allo-HSCT after relapse had significantly better OS than those without allo-HSCT treatment (median, 14.0 vs. 5.6 months, $P = 0.038$) (Supplementary Fig. 5).

Comparison of transcriptional signatures between patients with *DNMT3A*^{mut} and *DNMT3A*^{wt}

Gene expression profiles were compared between 80 patients with *DNMT3A*^{mut} and 184 patients with *DNMT3A*^{wt} and normal karyotypes. Hierarchical clustering was performed for the top DEGs to increase the clustering resolution (Fig. 3A). A total of 818 upregulated and 454 downregulated DEGs were identified between patients with *DNMT3A*^{mut} and *DNMT3A*^{wt} on the basis of a cutoff of |logFC|> 0.585 (absolute fold change >1.5 or <0.67) and $P < 0.05$. Several Hox family genes were among the top upregulated DEGs (Fig. 3B). Using the MsigDB Hallmark gene sets, we observed that the *DNMT3A*^{mut} transcriptome was enriched for TNFα signaling (normalized enrichment score ([NES] 3.89, FDR 3.85E−10), complement system (NES 3.34, FDR 3.85E−10), inflammatory response (NES 3.27, FDR 3.85E−10), and IL6/JAK/STAT3 signaling (NES 2.74, FDR 3.85E−10). The chemical and genetic perturbations (CGP) gene sets revealed the positive enrichment of several AML-related gene clusters, including the VERHAAK *NPM1*-mutated AML signature (NES 4.53, FDR 1.44E−9) and AML with aberrant cytoplasmic localization of *NPM1* (NES 3.80, FDR 1.44E−9) (Fig. 3C–E, Supplementary Table 6). In a subgroup analysis of 63 patients with *DNMT3A*^{mut} and normal karyotypes, the majority of originally identified DEGs remained significant (1215 of 1,272, 95.5%) (Fig. 3F).

To validate our RNA-seq data, we compared the transcriptomes of 40 patients with *DNMT3A*^{mut} and 59 patients with *DNMT3A*^{wt} and normal karyotypes in the TCGA cohort. Hallmark gene sets for TNFα signaling, the complement system, inflammatory response, and shared AML-related gene clusters in the CGP gene sets were among the primary enriched pathways. Further validation within the Beat-AML cohort revealed comparable results. These findings confirm the alignment between our RNA-seq data and that previously reported (Supplementary Figs. 6 and 7) and underscore the unique immune microenvironment in these patients.

Distinct transcriptomic pathways in patients with *DNMT3A*^{mut}/*NPM1*^{mut}/*FLT3*-ITD^{wt}/*TET2*^{mut}

We observed a correlation between *TET2*^{mut} and unfavorable outcomes in patients with *DNMT3A*^{mut}/*NPM1*^{mut}/*FLT3*-ITD^{wt} and further investigated whether these patients exhibited overlapping transcriptomic profiles. We compared the RNA-seq data between patients with *TET2*^{mut} ($n = 4$) and those with *TET2*^{wt} ($n = 25$) within the *DNMT3A*^{mut}/*NPM1*^{mut}/*FLT3*-ITD^{wt} subgroup. The *TET2*^{mut} group was identified as a distinct cluster through hierarchical clustering (Fig. 4A). Additionally, the principal component analysis plot effectively distinguished patients with *TET2*^{mut} from those with *TET2*^{wt}. By contrast, patients with *FLT3*-ITD, *NRAS*, and *PTPN11* mutations could not be clustered separately from those without these mutations (Supplementary Fig. 8A).

A total of 3801 DEGs were identified between the *TET2*^{mut} and *TET2*^{wt} groups (Fig. 4B and Supplementary Table 7). The number of DEGs between the *TET2*^{mut} and *TET2*^{wt} groups was notably higher than that between other mutated subgroups. Leukemic stem cell (LSC) signatures were enriched in the *TET2*^{mut} group (NES 2.42, FDR 1.47E-4), and genes downregulated in LSC were negatively enriched. An analysis of the MsigDB Hallmark and Gene Ontology Biological Process gene sets revealed significant negative enrichment of IL6/JAK/STAT3 signaling (NES −1.60, FDR 8.42E−3), pathways associated with dendritic cell migration (NES − 2.20, FDR 8.80E-5), and lymphocyte chemotaxis (NES −1.95, FDR 2.08E−3) (Fig. 4C–E and Supplementary Fig. 8B). The top DEGs included *MMP14* (logFC = 1.89), *CD200* (logFC = 1.39), *CT45A5* (logFC = –2.60), and *CT45A8* (logFC = –1.71) (Fig. 4F–G). *MMP14*, derived from mesenchymal stem cells, promotes AML progression and chemoresistance [32]. *CD200* is a novel LSC marker that can capture the entire LSC compartment from samples provided by patients with AML, including those with *NPM1* mutations [33]. The

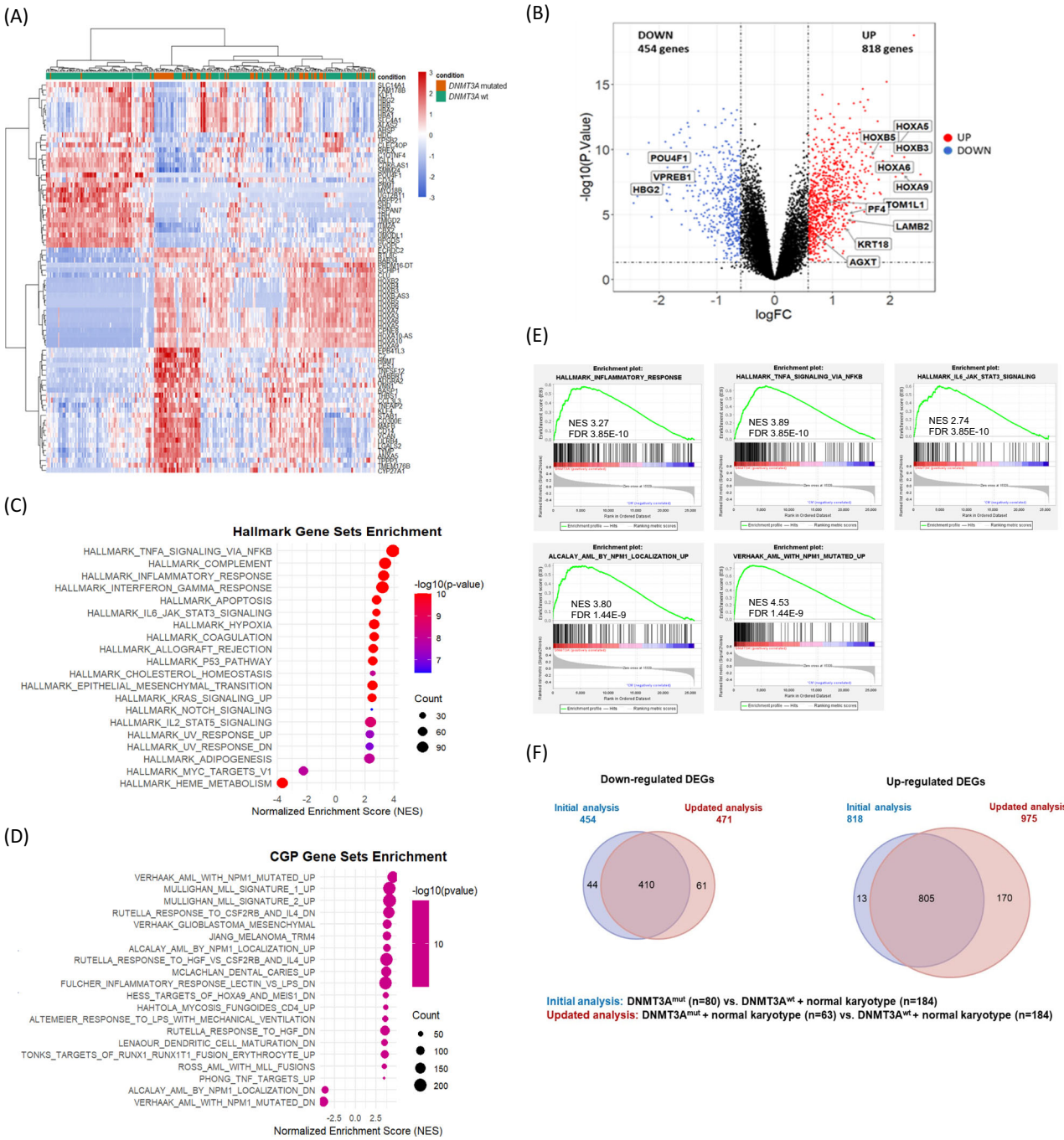

Fig. 3 Comparison of transcriptional signatures between patients with *DNMT3A*^{mut} and *DNMT3A*^{wt}. **A** Unsupervised hierarchical clustering of patients with *DNMT3A*^{mut} and *DNMT3A*^{wt} patients, with the major upregulated and downregulated DEGs displayed. Colors represent normalized gene expression values. **B** Volcano plot comparison of all RNA-seq genes between patients with *DNMT3A*^{mut} and *DNMT3A*^{wt}. Positive (logFC > 0) and negative (logFC < 0) fold changes indicate upregulated and downregulated genes, respectively, in patients with *DNMT3A*^{mut}. **C**, **D** Bubble plots illustrating a comparison of enriched and depleted MSigDB CGP and Hallmark gene sets between patients with *DNMT3A*^{mut} and *DNMT3A*^{wt}. Bubble size represents gene counts, and colors indicate statistical significance. **E** Gene Set Enrichment Analysis plots displaying overrepresentation of immune gene set signatures within the *DNMT3A*^{mut} transcriptome. **F** Venn diagram of DEGs identified in initial and updated comparisons between patients with *DNMT3A*^{mut} and *DNMT3A*^{wt}. An initial analysis included RNA-seq data from 80 patients with *DNMT3A*^{mut} and 184 with *DNMT3A*^{wt} and normal karyotypes. In an updated analysis, a subset of 63 *DNMT3A*^{mut} patients with normal karyotypes were compared with the original 184 patients with *DNMT3A*^{wt}.

CT45 gene family consists of 10 distinct but highly similar genes that are nearly identical at the protein level (*CT45A1–CT45A10*). CT45 peptides can induce CD8^{+} T cell activation through intracellular IFNγ staining [34].

To validate these results and strengthen the robustness of our data, we analyzed RNA-seq data from 40 patients with *DNMT3A*^{mut} in the TCGA AML cohort, 6 of whom had *TET2*^{mut}. Selected AML gene clusters, LSC signatures, and pathways related to dendritic cell migration were significantly enriched in patients with *TET2*^{mut} (Supplementary Fig. 9), in alignment with our findings. Additionally, *MMP14* and *CD200* were identified as DEGs in the TCGA cohort.

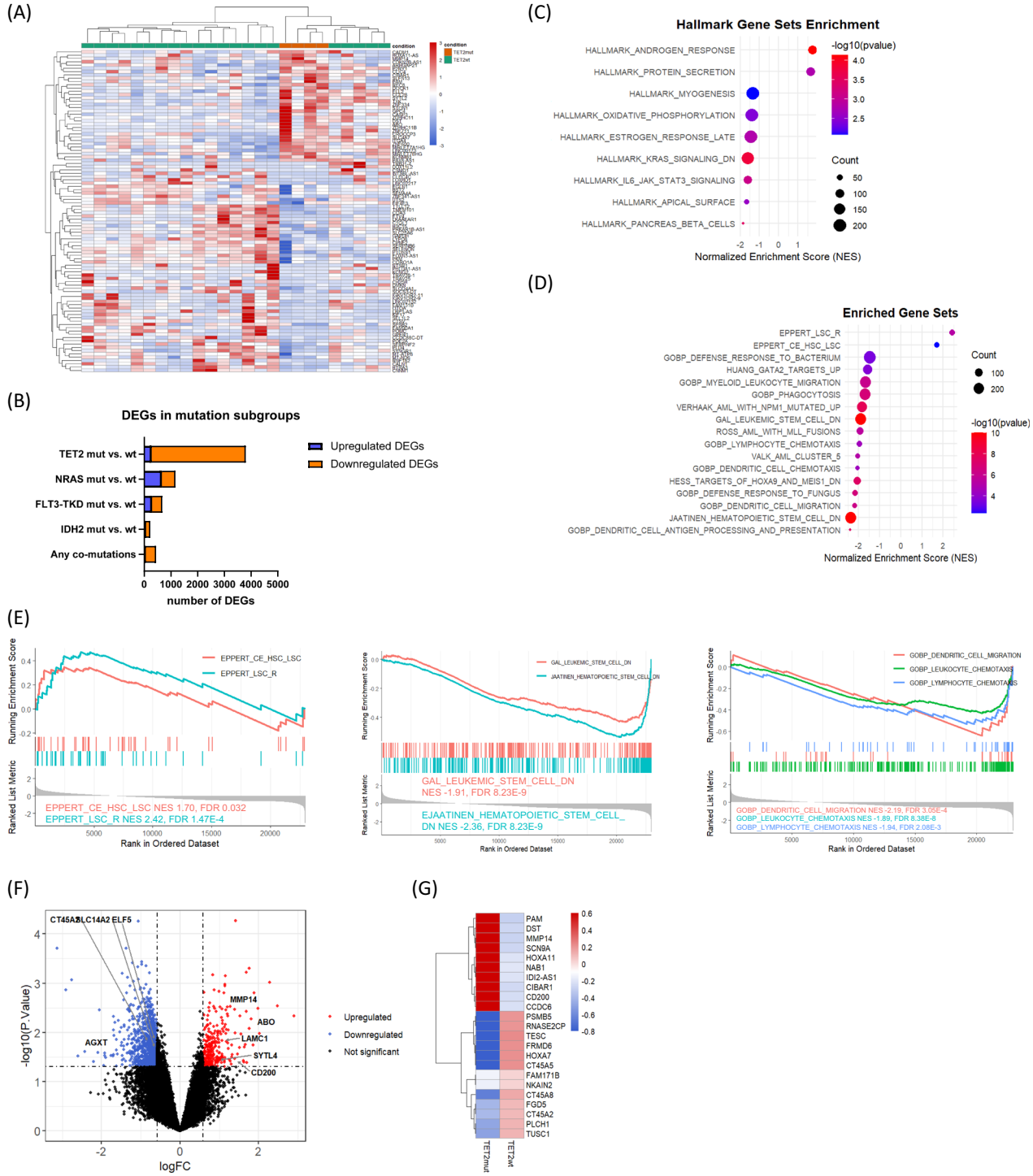

Fig. 4 Differential transcriptional signatures between patients with *TET2*^{mut} and *TET2*^{wt} within the *DNMT3A*^{mut}/*NPM1*^{mut}/*FLT3*-ITD^{wt} subgroup. A Unsupervised hierarchical clustering of *TET2*^{mut} and *TET2*^{wt} patients within the *DNMT3A*^{mut}/*NPM1*^{mut}/*FLT3*-ITD^{wt} subgroup, displaying the top upregulated and downregulated DEGs. Colors represented normalized gene expression values. **B** Number of upregulated and downregulated DEGs identified through comparison of transcriptomes in patients with AML with and without *TET2*, *FLT3*-TKD, *IDH2*, *NRAS* or any other co-mutations. Bubble plots illustrating enriched and depleted MSigDB Hallmark (**C**) and CGP and Gene Ontology Biological Processes gene sets (**D**) between patients with *TET2*^{mut} and *TET2*^{wt} in the *DNMT3A*^{mut}/*NPM1*^{mut}/*FLT3*-ITD^{wt} subgroup. Bubble size represents gene counts, and color indicates statistical significance. **E** Gene Set Enrichment Analysis plots indicating enrichment of LSC and immune gene set signatures within the *TET2*^{mut} transcriptome. **F**, **G** Volcano plot of DEGs with genes downregulated (logFC < 0) and upregulated (logFC > 0) in patients with *DNMT3A*^{mut}/*NPM1*^{mut}/*FLT3*-ITD^{wt} based on *TET2* mutation status. Key DEGs are highlighted in a heat map, with colors representing normalized gene expression values.

DISCUSSION

Our findings underscore the complexity of AML in patients with *DNMT3A*^{mut} and the prognostic implications of its associated molecular landscape. Patients with *DNMT3A*^{mut} were stratified into four subgroups on the basis of their *NPM1* and *FLT3*-ITD mutation status. All subgroups exhibited a poorer prognosis than that predicted under each designated ELN-2022 risk category. Additionally, within the *DNMT3A*^{mut}/*NPM1*^{mut}/*FLT3*-ITD^{wt} group, *TET2* mutations may have characterized a unique subgroup with distinct transcriptomic features and an unfavorable prognosis.

In previous studies, patients with *DNMT3A*^{mut} have exhibited inferior OS and EFS [1, 2, 35]. In our study, patients with *DNMT3A*^{mut} were stratified on the basis of their *NPM1* and *FLT3*-ITD mutation status, and the results indicated the profound prognostic implications of these co-mutations. The *DNMT3A*^{mut}/*NPM1*^{mut}/*FLT3*-ITD^{wt} subgroup trended toward worse outcomes than the ELN-2022 favorable risk group. These findings suggest that despite the traditional classification of the *NPM1*^{mut}/*FLT3*-ITD^{wt} subgroup as favorable, patients in this group with *DNMT3A*^{mut} may fall under a distinct intermediate risk category. The remaining three subgroups, *NPM1*^{mut}/*FLT3*-ITD^{mut}, *NPM1*^{wt}/*FLT3*-ITD^{mut}, and *NPM1*^{wt}/*FLT3*-ITD^{wt}, all exhibited poorer prognoses than the ELN-2022 intermediate risk group, aligning more closely with the ELN-2022 unfavorable risk criteria. These results highlight the heterogeneity within the *DNMT3A*^{mut} population and the need for more precise risk stratification. Our findings further underscore the critical role of allo-HSCT at CR1 in improving survival outcomes for patients with AML and *DNMT3A*^{mut}. Among all patients with AML and *DNMT3A*^{mut}, significantly better OS and DFS was observed in those who received allo-HSCT at CR1 than in those who received post-remission chemotherapy. Within the *DNMT3A*^{mut}/*NPM1*^{mut}/*FLT3*-ITD^{wt} subgroup, allo-HSCT at CR1 improved DFS, whereas OS remained comparable with other groups. Although we conducted Mantel–Byar analysis and constructed Simon–Makuch plots to address immortal time bias, further randomized studies are necessary to clarify the role of allo-HSCT in this patient population.

To better understand why worse outcomes were observed in the *DNMT3A*^{mut}/*NPM1*^{mut}/*FLT3*-ITD^{wt} subgroup than in ELN-2022 favorable risk patients, we investigated the effects of co-mutations within this subgroup. Combined *DNMT3A*^{mut} and *TET2*^{mut} in patients with AML and *NPM1*^{mut}/*FLT3*-ITD^{wt} resulted in a risk reclassification from ELN-favorable to intermediate, whereas patients without *TET2*^{mut} had survival more similar to patients in the ELN favorable risk group. Our study presents the novel finding that *TET2*^{mut} may adversely affect prognosis in patients with *DNMT3A*^{mut}/*NPM1*^{mut}/*FLT3*-ITD^{wt}. We refined the subgroup to exclude *PTPN11* and *IDH2* mutations, which further underscored the deleterious effects of *TET2*^{mut} on survival and disease progression. This finding was sufficiently validated in external cohorts. Among all patients with AML, *TET2*^{mut} have been associated with adverse prognosis [36–39]. In a recent study, two epigenetic modifiers, *TET2* and *DNMT3A*, synergistically induced leukemogenesis [40]. In a *DNMT3A* and *TET2* double-knockout mouse model, dysregulated self-renewal of hematopoietic stem cells may have caused hematological abnormalities. Both *DNMT3A* and *TET2* play key roles in repressing lineage-specific transcription factors in hematopoietic stem cells. The concurrent loss of both genes causes notable upregulation of downstream transcription factors, which eventually leads to malignant transformation [40]. In our study, patients with AML and *TET2*^{mut} formed a separated transcriptomic cluster within the *DNMT3A*^{mut}/*NPM1*^{mut}/*FLT3*-ITD^{wt} subgroup and exhibited the largest number of DEGs compared with patients with *TET2*^{wt}. Enrichment of LSC signatures may partly explain the poor outcomes observed in this group, and these results were validated in the TCGA cohort. Based on the distinct transcriptomic signatures, prognostic implications, reproducibility across cohorts, and functional evidence, *DNMT3A*^{mut}/*NPM1*^{mut}/*FLT3*-ITD^{wt}/*TET2*^{mut} AML can be redefined as a distinct subgroup to improve ELN classification systems and risk stratification.

Our study has several limitations. First, we relied on bulk BM aspirates for RNA-seq analysis. Further research incorporating single-cell RNA-seq or mass cytometry can elucidate the primary contributor among cell components. Second, although we validated the poor outcomes in patients with *DNMT3A*^{mut}/*NPM1*^{mut}/*FLT3*-ITD^{wt}/*TET2*^{mut} AML with external cohort data, this finding should be interpreted with caution due to the small size of the *TET2*^{mut} subgroup. Further studies remain necessary to ensure the reproducibility of our results. Third, all patients in our study received intensive chemotherapy, and the interaction of specific mutation groups with venetoclax and hypomethylating agents was not examined [41, 42]. Furthermore, most patients with *FLT3*-ITD did not receive *FLT3* inhibitor treatment before and after HSCT, potentially affecting their prognosis.

Our findings underscore the necessity of integrating genetic and transcriptomic analyses to comprehensively understand the heterogeneity of *DNMT3A*-mutated AML. Irrespective of *NPM1* and *FLT3*-ITD mutation status, poorer prognoses were observed among patients with AML and *DNMT3A*^{mut} than anticipated under the assigned ELN-2022 risk category. Patients with *TET2*^{mut} comprised a unique subgroup within the ELN-2022 favorable *DNMT3A*^{mut}/*NPM1*^{mut}/*FLT3*-ITD^{wt} group, characterized by distinct transcriptomic features and an unfavorable prognosis. This study provides a robust and comprehensive dataset of patient demographic characteristics, clinical outcomes, NGS, and RNA-seq information, offering valuable resources for future AML research.

DATA AVAILABILITY

Our RNA-seq data can be accessed online from the National Center for Biotechnology Information's Gene Expression Omnibus under GSE297413. Clinical and mutation data and computer codes with nonidentifiable patient information are accessible on reasonable request. The corresponding author (F.-M.T.) will evaluate the appropriateness of such requests.

REFERENCES

1. Ley TJ, Ding L, Walter MJ, McLellan MD, Lamprecht T, Larson DE, et al. *DNMT3A* Mutations in Acute Myeloid Leukemia. N Engl J Med. 2010;363:2424–33.
2. Hou HA, Kuo YY, Liu CY, Chou WC, Lee MC, Chen CY, et al. DNMT3A mutations in acute myeloid leukemia: stability during disease evolution and clinical implications. Blood. 2012;119:559–68.
3. Gaidzik VI, Schlenk RF, Paschka P, Stölzle A, Späth D, Kuendgen A, et al. Clinical impact of DNMT3A mutations in younger adult patients with acute myeloid leukemia: results of the AML Study Group (AMLSG). Blood. 2013;121:4769–77.
4. Papaemmanuil E, Gerstung M, Bullinger L, Gaidzik VI, Paschka P, Roberts ND, et al. Genomic Classification and Prognosis in Acute Myeloid Leukemia. N Engl J Med. 2016;374:2209–21.
5. Thol F, Damm F, Lüdeking A, Winschel C, Wagner K, Morgan M, et al. Incidence and Prognostic Influence of *DNMT3A* Mutations in Acute Myeloid Leukemia. J Clin Oncol. 2011;29:2889–96.
6. Renneville A, Boissel N, Nibourel O, Berthon C, Helevaut N, Gardin C, et al. Prognostic significance of DNA methyltransferase 3A mutations in cytogenetically normal acute myeloid leukemia: a study by the Acute Leukemia French Association. Leukemia. 2012;26:1247–54.
7. Marcucci G, Metzeler KH, Schwind S, Becker H, Maharry K, Mrózek K, et al. Age-Related Prognostic Impact of Different Types of *DNMT3A* Mutations in Adults With Primary Cytogenetically Normal Acute Myeloid Leukemia. J Clin Oncol. 2012;30:742–50.
8. Ribeiro AFT, Pratcorona M, Erpelinck-Verschueren C, Rockova V, Sanders M, Abbas S, et al. Mutant DNMT3A: a marker of poor prognosis in acute myeloid leukemia. Blood. 2012;119:5824–31.
9. Bezerra MF, Lima AS, Piqué-Borràs MR, Silveira DR, Coelho-Silva JL, Pereira-Martins DA, et al. Co-occurrence of DNMT3A, NPM1, FLT3 mutations identifies a subset of acute myeloid leukemia with adverse prognosis. Blood. 2020;135:870–5.
10. Loghavi S, Zuo Z, Ravandi F, Kantarjian HM, Bueso-Ramos C, Zhang L, et al. Clinical features of De Novo acute myeloid leukemia with concurrent DNMT3A, FLT3 and NPM1 mutations. J Hematol OncolJ Hematol Oncol. 2014;7:74.
11. Elrhman HAEA, El-Meligui YM, Elalawi SM. Prognostic Impact of Concurrent DNMT3A, FLT3 and NPM1 Gene Mutations in Acute Myeloid Leukemia Patients. Clin Lymphoma Myeloma Leuk. 2021;21:e960–9.
12. Döhner H, Wei AH, Appelbaum FR, Craddock C, DiNardo CD, Dombret H, et al. Diagnosis and management of AML in adults: 2022 recommendations from an international expert panel on behalf of the ELN. Blood. 2022;140:1345–77.

13. Wakita S, Marumo A, Morita K, Kako S, Toya T, Najima Y, et al. Mutational analysis of *DNMT3A* improves the prognostic stratification of patients with acute myeloid leukemia. Cancer Sci. 2023;114:1297–308.
14. Ostronoff F, Othus M, Ho PA, Kutny M, Geraghty DE, Petersdorf SH, et al. Mutations in the DNMT3A exon 23 independently predict poor outcome in older patients with acute myeloid leukemia: a SWOG report. Leukemia. 2013;27:238–41.
15. Arber DA, Orazi A, Hasserjian RP, Borowitz MJ, Calvo KR, Kvasnicka HM, et al. International Consensus Classification of Myeloid Neoplasms and Acute Leukemias: integrating morphologic, clinical, and genomic data. Blood. 2022;140:1200–28.
16. Khoury JD, Solary E, Abla O, Akkari Y, Alaggio R, Apperley JF, et al. The 5th edition of the World Health Organization Classification of Haematolymphoid Tumours: Myeloid and Histiocytic/Dendritic Neoplasms. Leukemia. 2022;36:1703–19.
17. Lo M, Tsai XC, Lin C, Tien F, Kuo Y, Lee W, et al. Validation of the prognostic significance of the 2022 European LEUKEMIANET risk stratification system in intensive chemotherapy treated aged 18 to 65 years patients with de novo acute myeloid leukemia. Am J Hematol. 2023;98:760–9.
18. Hou HA, Tsai CH, Lin CC, Chou WC, Kuo YY, Liu CY, et al. Incorporation of mutations in five genes in the revised International Prognostic Scoring System can improve risk stratification in the patients with myelodysplastic syndrome. Blood Cancer J. 2018;8:39.
19. Grimwade D, Walker H, Oliver F, Wheatley K, Harrison C, Harrison G, et al. The Importance of Diagnostic Cytogenetics on Outcome in AML: Analysis of 1,612 Patients Entered Into the MRC AML 10 Trial. Blood. 1998;92:2322–33.
20. Lee W, Lin C, Tsai C, Tseng M, Kuo Y, Liu M, et al. Effect of mutation allele frequency on the risk stratification of myelodysplastic syndrome patients. Am J Hematol. 2022;97:1589–98.
21. Tien FM, Yao CY, Tsai XCH, Lo MY, Chen CY, Lee WH, et al. Dysregulated immune and metabolic pathways are associated with poor survival in adult acute myeloid leukemia with CEBPA bZIP in-frame mutations. Blood Cancer J. 2024;14:15.
22. Dobin A, Davis CA, Schlesinger F, Drenkow J, Zaleski C, Jha S, et al. STAR: ultrafast universal RNA-seq aligner. Bioinformatics. 2013;29:15–21.
23. Frankish A, Diekhans M, Ferreira AM, Johnson R, Jungreis I, Loveland J, et al. GENCODE reference annotation for the human and mouse genomes. Nucleic Acids Res. 2019;47:D766–73.
24. Robinson MD, McCarthy DJ, Smyth GK. edgeR: a Bioconductor package for differential expression analysis of digital gene expression data. Bioinformatics. 2010;26:139–40.
25. Subramanian A, Tamayo P, Mootha VK, Mukherjee S, Ebert BL, Gillette MA, et al. Gene set enrichment analysis: A knowledge-based approach for interpreting genome-wide expression profiles. Proc Natl Acad Sci. 2005;102:15545–50.
26. Tien FM, Hou HA, Tsai CH, Tang JL, Chiu YC, Chen CY, et al. GATA2 zinc finger 1 mutations are associated with distinct clinico-biological features and outcomes different from GATA2 zinc finger 2 mutations in adult acute myeloid leukemia. Blood Cancer J. 2018;8:87.
27. Tyner JW, Tognon CE, Bottomly D, Wilmot B, Kurtz SE, Savage SL, et al. Functional genomic landscape of acute myeloid leukaemia. Nature. 2018;562:526–31.
28. The Cancer Genome Atlas Research Network. Genomic and Epigenomic Landscapes of Adult De Novo Acute Myeloid Leukemia. N Engl J Med. 2013;368:2059–74.
29. Tazi Y, Arango-Ossa JE, Zhou Y, Bernard E, Thomas I, Gilkes A, et al. Unified classification and risk-stratification in Acute Myeloid Leukemia. Nat Commun. 2022;13:4622.
30. Hou HA, Lin CC, Chou WC, Liu CY, Chen CY, Tang JL, et al. Integration of cytogenetic and molecular alterations in risk stratification of 318 patients with de novo non-M3 acute myeloid leukemia. Leukemia. 2014;28:50–8.
31. Simon R, Makuch RW. A non-parametric graphical representation of the relationship between survival and the occurrence of an event: application to responder versus non-responder bias. Stat Med. 1984;3:35–44.
32. Wu J, Liu X, Li X, Wang Q, Zhang N, Zhou F. Mesenchymal Stromal Cell-Derived MMP14 Facilitates Leukemia Progression and Chemotherapy Resistance. Blood. 2023;142:5993.
33. Ho JM, Dobson SM, Voisin V, McLeod J, Kennedy JA, Mitchell A, et al. CD200 expression marks leukemia stem cells in human AML. Blood Adv. 2020;4:5402–13.
34. Coscia F, Lengyel E, Duraiswamy J, Ashcroft B, Bassani-Sternberg M, Wierer M, et al. Multi-level Proteomics Identifies CT45 as a Chemosensitivity Mediator and Immunotherapy Target in Ovarian Cancer. Cell. 2018;175:159–170.e16.
35. Park DJ, Kwon A, Cho BS, Kim HJ, Hwang KA, Kim M, et al. Characteristics of *DNMT3A* mutations in acute myeloid leukemia. BLOOD Res. 2020;55:17–26.
36. Delhommeau F, Valle VD, Massé A, Couedic JPL, Lécluse Y, Marzac C, et al. Mutation in TET2 in Myeloid Cancers. N Engl J Med. 2009;360:2289–301.
37. Chou WC, Chou SC, Liu CY, Chen CY, Hou HA, Kuo YY, et al. TET2 mutation is an unfavorable prognostic factor in acute myeloid leukemia patients with intermediate-risk cytogenetics. Blood. 2011;118:3803–10.
38. Pan X, Chang Y, Ruan G, Zhou S, Jiang H, Jiang Q, et al. TET2 mutations contribute to adverse prognosis in acute myeloid leukemia (AML): results from a comprehensive analysis of 502 AML cases and the Beat AML public database. Clin Exp Med. 2024;24:35.
39. Metzeler KH, Maharry K, Radmacher MD, Mrózek K, Margeson D, Becker H, et al. *TET2* Mutations Improve the New European LeukemiaNet Risk Classification of Acute Myeloid Leukemia: A Cancer and Leukemia Group B Study. J Clin Oncol. 2011;29:1373–81.
40. Zhang X, Su J, Jeong M, Ko M, Huang Y, Park HJ, et al. DNMT3A and TET2 compete and cooperate to repress lineage-specific transcription factors in hematopoietic stem cells. Nat Genet. 2016;48:1014–23.
41. Itzykson R, Kosmider O, Cluzeau T, Mansat-De Mas V, Dreyfus F, Beyne-Rauzy O, et al. Impact of TET2 mutations on response rate to azacitidine in myelodysplastic syndromes and low blast count acute myeloid leukemias. Leukemia. 2011;25:1147–52.
42. Metzeler KH, Walker A, Geyer S, Garzon R, Klisovic RB, Bloomfield CD, et al. DNMT3A mutations and response to the hypomethylating agent decitabine in acute myeloid leukemia. Leukemia. 2012;26:1106–7.

ACKNOWLEDGEMENTS

We would like to express our thanks to the DNA Sequencing Core of the First Core Laboratory, National Taiwan University College of Medicine for their assistance with the experiments. This manuscript was edited by Wallace Academic Editing.

AUTHOR CONTRIBUTIONS

Contribution: S-CN was responsible for study design, literature collection, data management and interpretation, statistical analysis and manuscript writing; F-MT, Y-CY and X-CT were responsible for bioinformatics analysis; Y-YK, M-HT and L-IL were responsible for mutation analysis and interpretation; M-YL, C-YC, W-HL, C-CL, Y-SW, B-SK, M-Y, J-LT and W-CC contributed patient samples and clinical data; Y-LP, M-HT and M-CL performed the gene mutation and chromosomal studies. H-AH and H-FT coordinated the study and wrote and revised the manuscript. F-MT planned, designed, conceived and coordinated the study, analyzes the statistics and wrote and revised the manuscript. All authors provided final approval of the manuscript.

FUNDING

This work was partially sponsored by grants from the Ministry of Science and Technology (Taiwan) (MOST 104–2314-B-002–128-MY4, 106-2314-B-002-226-MY3, 108-2628-B-002-015, 109-2314-B-002-213, 111-2314-B-002-279 12-2314-B-002-197, and 113-2314-B-002-103), the Ministry of Health and Welfare (Taiwan) (MOHW 107-TDU-B-211-114009 and 111-TDU-B-221-114001).

COMPETING INTERESTS

The authors declare no competing interests.

ADDITIONAL INFORMATION

Supplementary information The online version contains supplementary material available at https://doi.org/10.1038/s41408-025-01287-9.

Correspondence and requests for materials should be addressed to Feng-Ming Tien.